

单箱双室筒支箱梁剪切变形及 剪力滞双重效应分析*

张 慧^{1,2}, 张玉元², 张元海², 李 巍³

- (1. 兰州交通大学 甘肃省道路桥梁与地下工程重点试验室, 兰州 730070;
2. 兰州交通大学 土木工程学院, 兰州 730070;
3. 西南交通大学, 成都 614202)

摘要: 基于各个翼板选取不同的最大剪切转角差为剪力滞广义位移,应用能量变分原理分别推导出了考虑和不考虑剪切变形时单箱双室截面控制微分方程组,结合边界条件给出了箱梁纵向应力和竖向挠度的初参数解,从力学、数学角度上证实了剪切变形和剪力滞效应是两个相对独立的力学行为,进一步阐述了二者对箱梁的影响,即剪切变形对箱梁截面纵向应力无影响,但是对竖向挠度有很大的影响.数值算例表明,利用该文解和数值解分析跨中截面剪力滞系数横向分布规律,二者吻合程度良好,其横向分布规律与单室箱梁类似,唯独不同之处是边腹板处的剪力滞效应比中腹板处的剪力滞效应略微大一些;挠度计算表明,剪切效应使得该箱梁在集中和均布荷载作用下跨中挠度分别增大4.6%和2.7%.

关键词: 双室箱梁; 剪力滞效应; 剪切变形; 能量变分法; 有限元

中图分类号: U441⁺.5 **文献标志码:** A

doi: 10.21656/1000-0887.370056

引 言

薄壁箱梁因其有利的受力特性而被广泛应用于现代桥梁工程中.薄壁箱梁发生竖向挠曲变形时,由腹板传递给翼缘板的剪力流使翼缘板在远离腹板处的纵向位移滞后于靠近腹板处的纵向位移,从而使箱梁翼缘板不满足平截面假设,这就是剪力滞效应^[1-2].

薄壁箱梁被广泛应用于桥梁上部结构设计当中,其设计和计算时必须考虑剪力滞效应这已是众所周知的^[1,3-5],但是要不要考虑剪切变形,以及剪切变形对剪力滞效应是否有影响需要进一步的论证和阐述.文献[6-9]以单室箱梁为例,假设纵向位移模式,应用能量变分原理获得了箱梁截面控制微分方程;文献[10]从箱梁刚度入手以等效刚度的形式分析了箱梁的剪切

* 收稿日期: 2016-02-26; 修订日期: 2016-04-15

基金项目: 国家自然科学基金(51508255; 51468032; 51268029); 长江学者和创新团队发展计划(IRT1139); 2015 人社部留学人员科技活动项目择优资助(西部寒冷地区正交异性钢箱梁-RPC 组合桥面基本力学性能研究)

作者简介: 张慧(1979—),女,副教授,博士(E-mail: 252757963@qq.com);

张玉元(1989—),男,硕士生(E-mail: 525040186@qq.com);

张元海(1965—),男,教授,博士,博士生导师(通讯作者. E-mail: zyh17012@163.com).

变形及剪力滞效应;文献[11]从弹性力学的角度出发推导了单室箱梁的纵向位移模式,应用能量变分原理导出截面控制微分方程,将剪切变形状态从全梁挠曲变形状态中分离出来,作为独立的变形状态进行分析;上述文献已经明确论述了剪切变形对剪力滞效应没有影响,即剪切变形不影响箱梁截面的纵向应力,但是,剪切变形对箱梁的竖向挠度影响很大,因此在桥梁设计中需考虑,目前大跨度、多室宽体箱梁已被广泛应用于实际桥梁建造中,考虑剪切变形对多室箱梁剪力滞效应的影响有待进一步从数学和力学角度出发,研究其受力机理和变形模式.本文将从这两个方面出发,应用能量变分原理推导出考虑和不考虑剪切变形的箱梁截面控制微分方程组,采用降阶法求得其通解,并结合相应的边界条件给出对应的闭合解,最后给出了箱梁竖向挠度的初参数解.以一个典型的单箱双室简支箱梁为例,验证本文分析方法的精确性,从数学和力学角度解释了剪切变形对箱梁纵向应力没有影响,但是对竖向挠度有很大的影响,因此在工程应用中需认真对待.

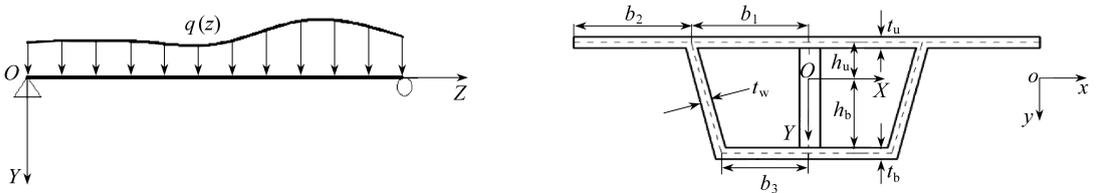
1 考虑剪切变形时单箱双室箱梁截面控制微分方程的推导及纵向应力、竖向挠度的解答

1.1 箱梁截面控制微分方程的推导

如图1所示, $OXYZ$ 为整体坐标系, $oxyz$ 为局部坐标系,箱梁在竖向任意荷载 $q(z)$ 作用下发生挠曲变形,选取最大剪切转角位移差作为剪力滞广义位移,则箱梁截面任意一点处的纵向位移为

$$u(x, y, z) = -y \cdot w'(z) + \omega_\zeta(x, y) \cdot U(z), \tag{1}$$

其中, $w(z)$ 为竖向挠度, $\omega_\zeta(x, y)$ 为翘曲位移函数, $U(z)$ 为最大剪切转角差;式中第一项为初等梁纵向位移,第二项为剪力滞引起的附加位移.



(a) 坐标系及荷载

(a) The coordinate system and load

(b) 横截面

(b) The cross section

图1 箱型截面简图

Fig. 1 Schematic of a box girder and its cross section

考虑剪切变形对剪力滞的影响,在对称竖向荷载作用下,中和轴的位置仍按初等梁理论确定,腹板变形考虑了 Timoshenko(铁摩辛柯)^[12]剪切变形理论.各个翼板的纵向位移表达式为:

顶板

$$u_1(x, y, z) = h_u \left[(w' - \beta) + \cos\left(\frac{\pi}{b_1}\left(x - \frac{b_1}{2}\right)\right) \cdot U_1(z) \right]; \tag{2}$$

悬臂板

$$u_2(x, y, z) = h_u \left[(w' - \beta) + \cos\frac{\pi x}{2b_2} \cdot U_2(z) \right]; \tag{3}$$

底板

$$u_3(x, y, z) = -h_b \left[(w' - \beta) + \cos\left(\frac{\pi}{b_3}\left(x - \frac{b_3}{2}\right)\right) \cdot U_3(z) \right]; \quad (4)$$

腹板

$$u_w = (w' - \beta)z, \quad (5)$$

其中, $\beta(z) = \alpha Q(z)/(GA)$, α 为剪切系数, $\alpha = A/A_w$, A 为箱梁截面面积, A_w 为箱梁截面腹板面积; $Q(z)$ 为箱梁某一截面处的剪力.

顶板、悬臂板、底板的应变能表达式为

$$\bar{U}_i = \frac{1}{2} \iiint (E\varepsilon_{i,z}^2 + G\gamma_{i,xz}^2) dx dy dz, \quad (6)$$

其中

$$\varepsilon_{i,z} = \frac{\partial u_i(x, y, z)}{\partial z}, \quad \gamma_{i,xz} \approx \frac{\partial u_i(x, y, z)}{\partial x}, \quad (7)$$

E 为弹性模量, G 为剪切模量.

令 $\phi(z) = w'(z) - \beta(z)$, 则可得箱梁各个翼板的应变能:

顶板应变能

$$\bar{U}_1 = EI_1 \int_0^l \left[\frac{1}{2} \phi'^2 + \frac{1}{4} U_1'^2 + \frac{2}{\pi} \phi' U_1' \right] dz + \frac{G\pi^2 I_1}{4b_1^2} \int_0^l U_1^2 dz; \quad (8)$$

悬臂板应变能

$$\bar{U}_2 = EI_2 \int_0^l \left[\frac{1}{2} \phi'^2 + \frac{1}{4} U_2'^2 + \frac{2}{\pi} \phi' U_2' \right] dz + \frac{G\pi^2 I_2}{16b_2^2} \int_0^l U_2^2 dz; \quad (9)$$

底板应变能

$$\bar{U}_3 = EI_3 \int_0^l \left[\frac{1}{2} \phi'^2 + \frac{1}{4} U_3'^2 + \frac{2}{\pi} \phi' U_3' \right] dz + \frac{G\pi^2 I_3}{4b_3^2} \int_0^l U_3^2 dz; \quad (10)$$

腹板应变能

$$\bar{U}_w = \frac{EI_w}{2} \int_0^l \phi'^2 dz + \frac{GA_w}{2} \int_0^l \beta^2 dz, \quad (11)$$

式中, I_i 为各个翼板的惯性矩, I_w 为腹板惯性矩; U_i 为各个翼板的最大剪切转角差, $i = 1$ 为顶板, $i = 2$ 为悬臂板, $i = 3$ 为底板.

外力势能

$$V = - \int_0^l qwdz; \quad (12)$$

箱梁总势能

$$\Pi = \bar{U}_1 + \bar{U}_2 + \bar{U}_3 + \bar{U}_w + V, \quad (13)$$

将式(8)~(12)代入式(13)可得

$$\begin{aligned} \Pi = & \frac{EI}{2} \int_0^l \phi'^2 dz + \frac{EI}{4} \int_0^l \sum_{i=1}^3 \alpha_i U_i'^2 dz + \frac{2EI}{\pi} \int_0^l \sum_{i=1}^3 \alpha_i \phi' U_i' dz + \\ & I \int_0^l \left(\frac{G\pi^2 \alpha_1}{4b_1^2} U_1^2 + \frac{G\pi^2 \alpha_2}{16b_2^2} U_2^2 + \frac{G\pi^2 \alpha_3}{4b_3^2} U_3^2 \right) dz + \frac{GA_w}{2} \int_0^l \beta^2 dz - \int_0^l qwdz, \end{aligned} \quad (14)$$

式中, $\alpha_i = I_i/I$, I 为箱梁截面抗弯惯性矩, q 为荷载集度.

将式(14)求一阶变分, 并令 $\delta\Pi = 0$, 则

$$\begin{aligned}
 \delta\Pi = & \int_0^l \left(EI\phi''' + \frac{2EI}{\pi} \sum_{i=1}^3 \alpha_i U_i''' - q \right) \delta w dz + \\
 & \int_0^l \left(\frac{G\pi^2 \alpha_1 I}{2b_1^2} U_1 - \frac{EI}{2} \alpha_1 U_1'' - \frac{2EI}{\pi} \alpha_1 \phi'' \right) \delta U_1 dz + \\
 & \int_0^l \left(\frac{G\pi^2 \alpha_2 I}{8b_2^2} U_2 - \frac{EI}{2} \alpha_2 U_2'' - \frac{2EI}{\pi} \alpha_2 \phi'' \right) \delta U_2 dz + \\
 & \int_0^l \left(\frac{G\pi^2 \alpha_3 I}{2b_3^2} U_3 - \frac{EI}{2} \alpha_3 U_3'' - \frac{2EI}{\pi} \alpha_3 \phi'' \right) \delta U_3 dz + \\
 & \int_0^l \left(EI\phi'' + \frac{2EI}{\pi} \sum_{i=1}^3 \alpha_i U_i'' + GA_w \beta \right) \delta \beta dz + \\
 & \left(EI\phi' + \frac{2EI}{\pi} \sum_{i=1}^3 \alpha_i U_i' \right) \delta w' \Big|_0^l - \left(EI\phi'' + \frac{2EI}{\pi} \sum_{i=1}^3 \alpha_i U_i'' \right) \delta w \Big|_0^l - \\
 & \left(EI\phi' + \frac{2EI}{\pi} \sum_{i=1}^3 \alpha_i U_i' \right) \delta \beta \Big|_0^l + \left(\frac{EI}{2} \sum_{i=1}^3 \alpha_i U_i' + \frac{2EI}{\pi} \sum_{i=1}^3 \alpha_i \phi' \right) \delta U_i \Big|_0^l = 0. \tag{15}
 \end{aligned}$$

根据变分引理,由式(15)可得截面控制微分方程

$$\phi''' + \frac{2}{\pi} \sum_{i=1}^3 \alpha_i U_i''' - \frac{q}{EI} = 0, \tag{16}$$

$$\frac{G\pi^2}{Eb_1^2} U_1 - U_1'' - \frac{4}{\pi} \phi'' = 0, \tag{17}$$

$$\frac{G\pi^2}{4Eb_2^2} U_2 - U_2'' - \frac{4}{\pi} \phi'' = 0, \tag{18}$$

$$\frac{G\pi^2}{Eb_3^2} U_3 - U_3'' - \frac{4}{\pi} \phi'' = 0, \tag{19}$$

$$\phi'' + \frac{2}{\pi} \sum_{i=1}^3 \alpha_i U_i'' + \frac{GA_w \beta}{EI} = 0, \tag{20}$$

$$\left(EI\phi' + \frac{2EI}{\pi} \sum_{i=1}^3 \alpha_i U_i' \right) \delta w' \Big|_0^l = 0, \tag{21}$$

$$\left(EI\phi'' + \frac{2EI}{\pi} \sum_{i=1}^3 \alpha_i U_i'' \right) \delta w \Big|_0^l = 0, \tag{22}$$

$$\left(EI\phi' + \frac{2EI}{\pi} \sum_{i=1}^3 \alpha_i U_i' \right) \delta \beta \Big|_0^l = 0, \tag{23}$$

$$\left(\frac{EI}{2} \sum_{i=1}^3 \alpha_i U_i' + \frac{2EI}{\pi} \sum_{i=1}^3 \alpha_i \phi' \right) \delta U_i \Big|_0^l = 0. \tag{24}$$

将式(16)积分一次

$$\phi'' = -\frac{2}{\pi} \sum_{i=1}^3 \alpha_i U_i'' - \frac{Q(z)}{EI}. \tag{25}$$

联立式(25)及式(16)~(24)消去 ϕ , 整理并写成矩阵的形式

$$\begin{bmatrix} U_1'' \\ U_2'' \\ U_3'' \end{bmatrix} = \frac{G\pi^2}{E(\pi^2 - 8\alpha_s)} \begin{bmatrix} \frac{\pi^2 - 8\alpha_2 - 8\alpha_3}{b_1^2} & \frac{8\alpha_2}{4b_2^2} & \frac{8\alpha_3}{b_3^2} \\ \frac{8\alpha_1}{b_1^2} & \frac{\pi^2 - 8\alpha_1 - 8\alpha_3}{4b_2^2} & \frac{8\alpha_3}{b_3^2} \\ \frac{8\alpha_1}{b_1^2} & \frac{8\alpha_2}{4b_2^2} & \frac{\pi^2 - 8\alpha_1 - 8\alpha_2}{b_3^2} \end{bmatrix} \begin{bmatrix} U_1 \\ U_2 \\ U_3 \end{bmatrix} + \frac{4\pi Q(z)}{EI(\pi^2 - 8\alpha_s)} \begin{bmatrix} 1 \\ 1 \\ 1 \end{bmatrix}, \quad (26)$$

其中 $\alpha_s = \alpha_1 + \alpha_2 + \alpha_3$.

1.2 微分方程组的边界条件及闭合解

对于式(26)的求解,采用降阶法^[13]得到一阶线性非齐次微分方程组,按照惯用的方法先求得齐次微分方程组的通解,再求出非齐次微分方程组的特解,然后将二者叠加得到非齐次微分方程组的通解,利用各自的边界条件得到相应的闭合解。

1.2.1 微分方程组的求解

1) 箱梁受集中力如图 2(a)所示

当 $0 \leq z \leq a$ 时

$$U_i = \bar{U}_i + U_i^* = \sum_{j=1,3,5} \varepsilon_{ij} (C_j \text{ch}(\lambda_j z) + C_{j+1} \text{sh}(\lambda_j z)) - \frac{2p}{GI\pi^3} m_i \quad (i = 1, 2, 3), \quad (27)$$

其中
$$\begin{bmatrix} m_1 \\ m_2 \\ m_3 \end{bmatrix} = \begin{bmatrix} b_1^2 \\ 4b_2^2 \\ b_3^2 \end{bmatrix}.$$

求一阶导数

$$U_i' = (\bar{U}_i + U_i^*)' = \sum_{j=1,3,5} \varepsilon_{ij} \lambda_j (C_j \text{sh}(\lambda_j z) + C_{j+1} \text{ch}(\lambda_j z)) \quad (i = 1, 2, 3). \quad (28)$$

当 $a \leq z \leq l$ 时,

$$U_i = \bar{U}_i + U_i^* = \sum_{j=1,3,5} \varepsilon_{ij} (C_j \text{ch}(\lambda_j z) + C_{j+1} \text{sh}(\lambda_j z)) + \frac{2p}{GI\pi^3} m_i \quad (i = 1, 2, 3). \quad (29)$$

求一阶导数

$$U_i' = (\bar{U}_i + U_i^*)' = \sum_{j=1,3,5} \varepsilon_{ij} \lambda_j (C_j \text{sh}(\lambda_j z) + C_{j+1} \text{ch}(\lambda_j z)) \quad (i = 1, 2, 3). \quad (30)$$

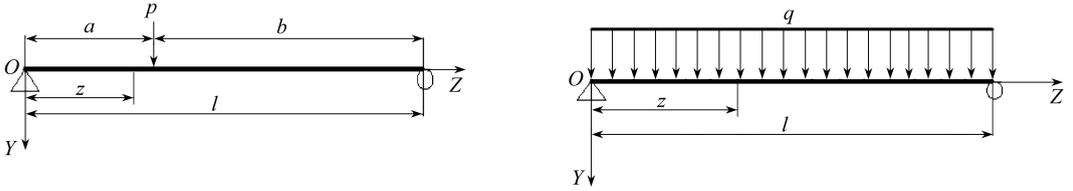
2) 箱梁受满跨均布力如图 2(b)所示

$$U_i = \bar{U}_i + U_i^* = \sum_{j=1,3,5} \varepsilon_{ij} (C_j \text{ch}(\lambda_j z) + C_{j+1} \text{sh}(\lambda_j z)) + \frac{2q}{GI\pi^3} (2z - l) m_i \quad (i = 1, 2, 3). \quad (31)$$

求一阶导数

$$U_i' = (\bar{U}_i + U_i^*)' = \sum_{j=1,3,5} \varepsilon_{ij} \lambda_j (C_j \text{sh}(\lambda_j z) + C_{j+1} \text{ch}(\lambda_j z)) + \frac{4q}{GI\pi^3} m_i \quad (i = 1, 2, 3), \quad (32)$$

式中, $\lambda_j, \varepsilon_{ij}$ 可以按照文献[13]介绍的方法将式(26)降阶化成6个一阶线性微分方程, λ_j 是由这6个常系数齐次线性微分方程构成的方程组的特征值; ε_{ij} 为 λ_j 所对应的方程组的特征向量。



(a) 简支梁集中力图示 (b) 简支梁均布力图示
 (a) The simply-supported beam under a concentrated force (b) The simply-supported beam under uniform force

图2 简支梁计算简图

Fig. 2 The calculation diagram of the simply-supported beam

1.2.2 边界条件

1) 集中力

$$U'_i|_{z=0} = 0, U'_i|_{z=l} = 0, U'_i|_{z=a}^+ = U'_i|_{z=a}^-, U_i|_{z=a}^+ = U_i|_{z=a}^-.$$

2) 均布力

$$U'_i|_{z=0} = 0, U'_i|_{z=l} = 0.$$

1.2.3 箱梁纵向应力解

求得各个翼板的最大剪切转角差, 由弹性力学原理即可获得各个翼板的纵向应力表达式:

顶板

$$\sigma_1 = Eh_u \left[-\frac{2}{\pi} \sum_{i=1}^3 \alpha_i U'_i - \frac{M}{EI} + U'_1 \cdot \cos\left(\frac{\pi}{b_1} \left(x - \frac{b_1}{2}\right)\right) \right]; \tag{33}$$

悬臂板

$$\sigma_2 = Eh_u \left[-\frac{2}{\pi} \sum_{i=1}^3 \alpha_i U'_i - \frac{M}{EI} + U'_2 \cdot \cos\frac{\pi x}{2b_2} \right]; \tag{34}$$

底板

$$\sigma_3 = -Eh_b \left[-\frac{2}{\pi} \sum_{i=1}^3 \alpha_i U'_i - \frac{M}{EI} + U'_3 \cdot \cos\left(\frac{\pi}{b_3} \left(x - \frac{b_3}{2}\right)\right) \right]. \tag{35}$$

1.2.4 箱梁竖向挠度解

先对式(25)积分两次, 积分时由于 $Q(z)$ 形式不同, 应该分跨中集中力和满跨均布力分别求解:

1) 跨中集中力下任意位置处的竖向挠度解

$$\phi'' = -\frac{2}{\pi} \sum_{i=1}^3 \alpha_i \left(\sum_{j=1,3,5} \varepsilon_{ij} \lambda_j^2 (C_j \text{ch}(\lambda_j z) + C_{j+1} \text{sh}(\lambda_j z)) \right) - \frac{p}{2EI} \tag{36}$$

$$\left(0 \leq z \leq \frac{l}{2} \right),$$

式(36)积分两次

$$\phi = -\frac{2}{\pi} \sum_{i=1}^3 \alpha_i \left(\sum_{j=1,3,5} \varepsilon_{ij} (C_j \text{ch}(\lambda_j z) + C_{j+1} \text{sh}(\lambda_j z)) \right) - \frac{pz^2}{4EI} + C_7 z + C_8 \tag{37}$$

$$\left(0 \leq z \leq \frac{l}{2} \right),$$

由边界条件 $\phi'(0) = 0$ 可得系数 C_7 .

由 $\phi(z) = w'(z) - \beta(z)$ 可得

$$w' = -\frac{2}{\pi} \sum_{i=1}^3 \alpha_i \left(\sum_{j=1,3,5} \varepsilon_{ij} (C_j \text{ch}(\lambda_j z) + C_{j+1} \text{sh}(\lambda_j z)) \right) - \frac{\rho z^2}{4EI} + \frac{\alpha p}{2GA} + C_7 z + C_8 \quad \left(0 \leq z \leq \frac{l}{2} \right), \quad (38)$$

式(38)积分一次

$$w = -\frac{2}{\pi} \sum_{i=1}^3 \alpha_i \left(\sum_{j=1,3,5} \frac{\varepsilon_{ij}}{\lambda_j} (C_j \text{sh}(\lambda_j z) + C_{j+1} \text{ch}(\lambda_j z)) \right) - \frac{\rho z^3}{12EI} + \frac{\alpha p z}{2GA} + \frac{C_7}{2} z^2 + C_8 z + C_9 \quad \left(0 \leq z \leq \frac{l}{2} \right), \quad (39)$$

由边界条件 $w|_{z=0} = 0, w'|_{z=l/2} = 0$, 可以得到系数 C_8, C_9 , 由此即可得到箱梁竖向挠度解。

2) 满跨均布力下任意位置处的竖向挠度解

$$\phi'' = -\frac{2}{\pi} \sum_{j=1,3,5} \varepsilon_{ij} \lambda_j^2 (C_j \text{ch}(\lambda_j z) + C_{j+1} \text{sh}(\lambda_j z)) - \frac{q(l-2z)}{2EI}, \quad (40)$$

式(40)积分两次

$$\phi = -\frac{2}{\pi} \sum_{j=1,3,5} \varepsilon_{ij} (C_j \text{ch}(\lambda_j z) + C_{j+1} \text{sh}(\lambda_j z)) - \frac{qz^2(3l-2z)}{12EI} + C_7 z + C_8, \quad (41)$$

由边界条件 $\phi'(0) = 0$, 可得系数 C_7 .

由 $\phi(z) = w'(z) - \beta(z)$ 可得

$$w' = -\frac{2}{\pi} \sum_{j=1,3,5} \varepsilon_{ij} (C_j \text{ch}(\lambda_j z) + C_{j+1} \text{sh}(\lambda_j z)) - \frac{qz^2(3l-2z)}{12EI} + \frac{\alpha q(l-2z)}{2GA} + C_7 z + C_8, \quad (42)$$

式(42)积分一次

$$w = -\frac{2}{\pi} \sum_{j=1,3,5} \frac{\varepsilon_{ij}}{\lambda_j} (C_j \text{sh}(\lambda_j z) + C_{j+1} \text{ch}(\lambda_j z)) - \frac{qz^3(2l-z)}{24EI} + \frac{\alpha qz(l-z)}{2GA} + \frac{C_7}{2} z^2 + C_8 z + C_9, \quad (43)$$

由边界条件 $w|_{z=0} = 0, w'|_{z=l/2} = 0$, 可以得到系数 C_8, C_9 , 由此即可得到箱梁竖向挠度解。

2 不考虑剪切变形时单箱双室箱梁截面控制微分方程的推导及纵向应力、竖向挠度的解答

2.1 箱梁截面控制微分方程的推导

如图 1 所示的箱梁截面示意图, 由式(1)可以给出箱梁各个翼板的纵向位移表达式:

顶板

$$u_1(x, y, z) = h_u \left[w'(z) + \cos\left(\frac{\pi}{b_1} \left(x - \frac{b_1}{2}\right)\right) \cdot U_1(z) \right]; \quad (44)$$

悬臂板

$$u_2(x, y, z) = h_u \left[w'(z) + \cos\frac{\pi x}{2b_2} \cdot U_2(z) \right]; \quad (45)$$

底板

$$u_3(x, y, z) = -h_b \left[w'(z) + \cos\left(\frac{\pi}{b_3}\left(x - \frac{b_3}{2}\right)\right) \cdot U_3(z) \right]. \tag{46}$$

由式(6)、(7)、(13)可得箱梁总势能

$$\begin{aligned} \Pi = & \int_0^l \left(\frac{1}{2} EI w''^2 + M w'' \right) dz + \int_0^l \frac{EI}{4} \sum_{i=1}^3 \alpha_i U_i'^2 dz + \\ & \int_0^l \frac{2EI}{\pi} w'' \sum_{i=1}^3 \alpha_i U_i' dz + \int_0^l G \pi^2 I \left(\frac{\alpha_1 U_1^2}{4b_1^2} + \frac{\alpha_2 U_2^2}{16b_2^2} + \frac{\alpha_3 U_3^2}{4b_3^2} \right) dz. \end{aligned} \tag{47}$$

将式(47)求一阶变分,并令 $\delta\Pi = 0$, 则

$$\begin{aligned} \delta\Pi = & EI \int_0^l \left(w'' + \frac{2}{\pi} \sum_{i=1}^3 \alpha_i U_i' + \frac{M}{EI} \right) \delta w'' dz + EI \left[\sum_{i=1}^3 \left(\frac{1}{2} \alpha_i U_i' + \frac{2}{\pi} \alpha_i w'' \right) \delta U_i \right] \Big|_0^l + \\ & \int_0^l \left(G \pi^2 \left(\frac{I_1 U_1}{2b_1^2} \delta U_1 + \frac{I_2 U_2}{8b_2^2} \delta U_2 + \frac{I_3 U_3}{2b_3^2} \delta U_3 \right) - \right. \\ & \left. \frac{EI}{2} \sum_{i=1}^3 \alpha_i U_i'' \delta U_i - \frac{2EI}{\pi} \sum_{i=1}^3 \alpha_i w''' \delta U_i \right) dz = 0. \end{aligned} \tag{48}$$

根据变分引理,由式(48)可得截面控制微分方程

$$w'' + \frac{2}{\pi} \sum_{i=1}^3 \alpha_i U_i' + \frac{M}{EI} = 0, \tag{49}$$

$$\sum_{i=1}^3 \left[\left(\frac{1}{2} \alpha_i U_i' + \frac{2}{\pi} \alpha_i w'' \right) \delta U_i \right] \Big|_0^l = 0, \tag{50}$$

$$\frac{G \pi^2}{E b_1^2} U_1 - U_1'' - \frac{4}{\pi} w''' = 0, \tag{51}$$

$$\frac{G \pi^2}{4 E b_2^2} U_2 - U_2'' - \frac{4}{\pi} w''' = 0, \tag{52}$$

$$\frac{G \pi^2}{E b_3^2} U_3 - U_3'' - \frac{4}{\pi} w''' = 0. \tag{53}$$

整理式(49)、(51)~(53),并写成矩阵的形式

$$\begin{aligned} \begin{bmatrix} U_1'' \\ U_2'' \\ U_3'' \end{bmatrix} = & \frac{G \pi^2}{E(\pi^2 - 8\alpha_s)} \begin{bmatrix} \pi^2 - 8\alpha_2 - 8\alpha_3 & \frac{8\alpha_2}{4b_2^2} & \frac{8\alpha_3}{b_3^2} \\ \frac{8\alpha_1}{b_1^2} & \pi^2 - 8\alpha_1 - 8\alpha_3 & \frac{8\alpha_3}{b_3^2} \\ \frac{8\alpha_1}{b_1^2} & \frac{8\alpha_2}{4b_2^2} & \pi^2 - 8\alpha_1 - 8\alpha_2 \end{bmatrix} \begin{bmatrix} U_1 \\ U_2 \\ U_3 \end{bmatrix} + \\ & \frac{4\pi Q(z)}{EI(\pi^2 - 8\alpha_s)} \begin{bmatrix} 1 \\ 1 \\ 1 \end{bmatrix}. \end{aligned} \tag{54}$$

此时,式(54)和式(26)相同,在考虑剪切变形和不考虑剪切变形时得到的截面控制微分方程组是相同的,简支边界条件下,其解也是相同的。

2.2 箱梁纵向应力解及竖向挠度解

关于微分方程组(54)的解法在式(27)~(32)中已经做出了详细的解答,此处不再赘述。

2.2.1 纵向应力解

各个翼板的纵向应力解如式(33)~(35),由此可以看出剪切变形不影响纵向应力,也不影响剪力滞效应,即剪切变形和剪力滞效应是两种独立的力学行为。

2.2.2 竖向挠度解

由式(49)可得

$$w'' = -\frac{2}{\pi} \sum_{i=1}^3 \alpha_i U'_i - \frac{M}{EI}. \quad (55)$$

1) 跨中集中力下任意位置处的竖向挠度解

$$w'' = -\frac{2}{\pi} \sum_{i=1}^3 \alpha_i \left(\sum_{j=1,3,5} \varepsilon_{ij} \lambda_j (C_j \text{sh}(\lambda_j z) + C_{j+1} \text{ch}(\lambda_j z)) \right) - \frac{pz}{2EI} \quad \left(0 \leq z \leq \frac{l}{2} \right), \quad (56)$$

式(56)两次积分可得

$$w = -\frac{2}{\pi} \sum_{i=1}^3 \alpha_i \left(\sum_{j=1,3,5} \frac{\varepsilon_{ij}}{\lambda_j} (C_j \text{sh}(\lambda_j z) + C_{j+1} \text{ch}(\lambda_j z)) \right) - \frac{pz^3}{12EI} + C_7 z + C_8 \quad \left(0 \leq z \leq \frac{l}{2} \right), \quad (57)$$

由边界条件 $w|_{z=0} = 0, w'|_{z=l/2} = 0$ 可得系数 C_7, C_8 。

2) 满跨均布力下任意位置处的竖向挠度解

$$w'' = -\frac{2}{\pi} \sum_{i=1}^3 \alpha_i \left(\sum_{j=1,3,5} \varepsilon_{ij} \lambda_j (C_j \text{sh}(\lambda_j z) + C_{j+1} \text{ch}(\lambda_j z)) + \frac{4q}{GI\pi^3} m_i \right) - \frac{qz(l-z)}{2EI}, \quad (58)$$

式(58)两次积分可得

$$w = -\frac{2}{\pi} \sum_{i=1}^3 \alpha_i \left(\sum_{j=1,3,5} \frac{\varepsilon_{ij}}{\lambda_j} (C_j \text{sh}(\lambda_j z) + C_{j+1} \text{ch}(\lambda_j z)) + \frac{2qz^2}{GI\pi^3} m_i \right) - \frac{qz^3}{12EI} \left(l - \frac{z}{2} \right) + C_7 z + C_8, \quad (59)$$

由边界条件 $w|_{z=0} = 0, w'|_{z=l/2} = 0$ 可得系数 C_7, C_8 。

3 算例

3.1 算例基本概况

以文献[14]跨度 50 m 的混凝土单箱双室简支箱梁为例,截面尺寸、测点位置见图 3,材料弹性模量 $E = 3.1 \times 10^4$ MPa, Poisson(泊松)比 $\mu = 1/6$ 。

1) 跨中集中力荷载 $p = 20$ kN;

2) 满跨均布力荷载 $q = 2$ kN/m。

3.2 箱梁跨中截面剪力滞系数横向分布规律

应用本文获得的各个翼板的纵向应力解研究跨中截面的剪力滞系数横向分布规律,同时利用 ANSYS-shell63 单元建立有限元模型并获得数值解,以 ANSYS 数值解为参照,分析本文建立箱梁纵向应力表达式的精确性和合理性。

分析箱梁跨中截面剪力滞横向分布规律,如表 1。

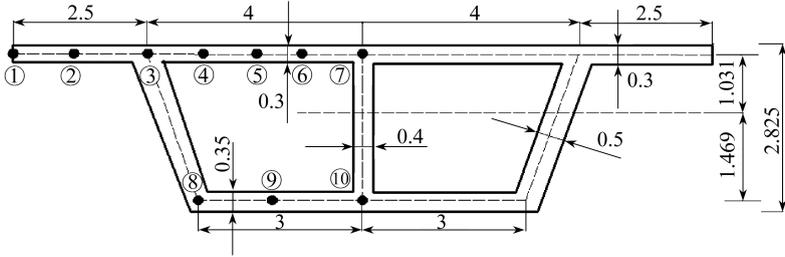


图3 截面尺寸及测点(尺寸单位: m)

Fig. 3 The cross section sizes(unit: m)

表 1 简支梁跨中截面测点剪力滞系数

Table 1 The shear lag coefficient of the cross section of the simply-supported beam

measuring point position		concentrated force			uniform force		
		present result	ANSYS result	error $\delta_1/\%$	present result	ANSYS result	error $\delta_2/\%$
cantilever plate	①	0.887	0.882	0.57	0.982	0.989	-0.71
	②	0.942	0.964	-2.28	0.989	0.997	-0.80
side web	③	1.074	1.143	-6.04	1.007	1.012	-0.49
	④	0.963	1.053	-8.55	0.996	1.004	-0.79
roof	⑤	0.916	1.019	-10.12	0.991	1.003	-1.20
	⑥	0.963	1.047	-8.02	0.996	1.007	-1.09
medium web	⑦	1.074	1.096	-2.01	1.007	1.017	-0.98
	⑧	1.074	1.054	1.89	1.015	1.045	-2.87
floor	⑨	0.975	1.003	-2.79	0.998	0.864	15.50
	⑩	1.074	1.025	4.78	1.015	1.039	-2.31

注 误差比 $\delta = (\text{本文解} - \text{ANSYS 解}) / \text{ANSYS 解} \times 100\%$

Note the error ratio $\delta = (\text{present solution} - \text{ANSYS solution}) / \text{ANSYS solution} \times 100\%$

由表 1 可以看出:集中力作用时,跨中截面测点剪力滞系数误差比基本在 $-8.55\% \sim -2.79\%$, $0.57\% \sim 4.78\%$;均布力作用时,跨中截面测点剪力滞系数误差比基本在 $-2.87\% \sim -0.49\%$;极少数测点误差比较大的原因是由于 ANSYS 建立有限元模型提取跨中截面测点应力值时应力集中影响结果偏大,但对分析箱梁横向分布规律几乎不受影响;分析证实了本文理论的精确性。顶板、底板与腹板交汇处表现为正剪力滞,其他测点表现为负剪力滞;集中力下的剪力滞效应更明显于均布力下的剪力滞效应;这些规律与单室箱梁类似。此外由 ANSYS 数值解可以看出,边腹板处的剪力滞系数略大于中腹板处的剪力滞系数。

3.3 挠度

采用图 3 所示的箱梁截面尺寸及跨度,分别从不考虑剪切变形、考虑剪切变形、初等梁理论^[15]入手分析箱梁的竖向挠度解,并对比三者之间的关系,分析考虑剪切变形对挠度的影响程度。

沿着跨度方向每隔 5 m 取箱梁底板与中腹板交汇处的测点为挠度测点,利用本文解、ANSYS 数值解来分析箱梁受集中力荷载和均布力荷载时箱梁的竖向挠度,如表 2 所示。

由表 2 可以看出:集中力作用时,不考虑剪切变形的挠度误差比在 $0.58\% \sim 1.40\%$,考虑剪切变形的挠度误差比在 $1.04\% \sim 5.59\%$;均布力作用时,不考虑剪切变形的挠度误差比在 $0.63\% \sim 0.88\%$,考虑剪切变形的挠度误差比在 $3.37\% \sim 4.03\%$ 。在集中力荷载分别作用下,不考虑和考虑剪切变形对跨中挠度分别增大 0.66% , 5.26% ;在均布力荷载分别作用下,不考虑和

考虑剪切变形对跨中挠度分别增大 0.63%, 3.37%; 在集中力和均布力荷载分别作用下, 考虑双重效应的跨中挠度比只考虑剪力滞效应的跨中挠度分别增大 4.6%, 2.7% (跨中截面=1 不考虑剪切变形挠度解-考虑剪切变形挠度解)÷不考虑剪切变形挠度解)。

表 2 挠度解

Table 2 The deflection solutions

position	elementary beam theory	concentrated force				elementary beam theory	uniform force			
		without shear		with shear			without shear		with shear	
		deflection		deflection			deflection		deflection	
		deflection	error $\delta_{11}/\%$	deflection	error $\delta_{12}/\%$		deflection	error $\delta_{21}/\%$	deflection	error $\delta_{22}/\%$
0	0	0	-	0	-	0	0	-	0	-
5	0.044 9	0.045 3	0.89	0.046 2	2.90	0.149	0.15	0.67	0.155	4.03
10	0.086 3	0.086 8	0.58	0.087 2	1.04	0.282	0.284	0.71	0.292	3.55
15	0.12	0.121	0.83	0.124	3.33	0.386	0.389	0.78	0.4	3.63
20	0.143	0.145	1.40	0.151	5.59	0.452	0.456	0.88	0.468	3.54
25	0.152	0.153	0.66	0.16	5.26	0.475	0.478	0.63	0.491	3.37
30	0.143	0.145	1.40	0.151	5.59	0.452	0.456	0.88	0.468	3.54
35	0.12	0.121	0.83	0.124	3.33	0.386	0.389	0.78	0.4	3.63
40	0.086 3	0.086 8	0.58	0.087 2	1.04	0.282	0.284	0.71	0.292	3.55
45	0.044 9	0.045 3	0.89	0.046 2	2.90	0.149	0.15	0.67	0.155	4.03
50	0	0		0		0	0		0	

注 误差比=(是否考虑剪切变形解-初等梁理论解)/初等梁理论解×100%

Note the error ratio=(present solution-elementary solution)/elementary solution×100%

同时也可以看出这三者之间的明显关系:考虑剪切变形的挠度解最大,不考虑剪切变形的挠度解次之,初等梁理论获得的挠度解最小。

4 结 论

结合算例单箱双室简支梁桥,分析可以得出以下结论:

1) 单箱双室简支箱梁剪力滞横向分布规律:顶板,由腹板处向箱室顶板中心递减;悬臂板,由腹板处向悬臂自由端递减;底板,由腹板向箱室底板中心递减。顶板、底板与腹板交汇处表现为正剪力滞效应,箱室顶板、底板中心表现为负剪力滞效应;此外,边腹板处剪力滞效应略大于中腹板处剪力滞效应。

2) 考虑剪切变形时的挠度比不考虑剪切变形时的挠度有明显的增加,剪切变形产生的竖向挠度大于剪力滞产生的竖向挠度,针对于本算例而言,在集中力和均布力荷载分别作用下,考虑双重效应的跨中挠度比只考虑剪力滞效应的跨中挠度分别增大 4.6% 和 2.7%, 同时也可得知考虑剪切变形的挠度解最大, 不考虑剪切变形的挠度解次之, 初等梁理论获得的挠度解最小。

3) 基于能量变分原理,推导了考虑剪切变形和不考虑剪切变形的双室箱梁截面控制微分方程组,结合相应的边界条件导出了各个翼板的纵向应力初参数解和挠度初参数解,从力学和数学的角度进一步阐释了剪切变形和剪力滞效应是两种相对独立的力学行为,考虑不考虑剪切变形对箱梁纵向应力没有任何影响,但是对竖向挠度有很大的影响,不容忽视,因此在多室箱梁设计中,应充分考虑剪切变形对竖向挠度的影响。

致谢 作者感谢兰州交通大学青年基金的资助。

参考文献(References):

- [1] 张元海, 胡玉茹, 林丽霞. 基于修正翘曲位移模式的薄壁箱梁剪力滞效应分析[J]. 土木工程学报, 2015, **48**(6): 44-45. (ZHANG Yuan-hai, HU Yu-ru, LIN Li-xia. Analysis on shear lag effect of thin-walled box girders based on a modified warping displacement mode[J]. *China Civil Engineering Journal*, 2015, **48**(6): 44-45. (in Chinese))
- [2] Visnjic G, Nozak D, Kosel F, Kosel T. Shear-lag influence on maximum specific bending stiffness and strength of composite I-beam wing spar[J]. *Journal of Aerospace Engineering*, 2011, **225**(5): 501-511.
- [3] Fabrizio G, Gianluca R, Graziano L. Partial interaction analysis with shear-lag effects of composite bridges; a finite element implementation for design applications[J]. *Advanced Steel Construction*, 2011, **7**(1): 1-16.
- [4] ZHANG Yuan-hai. Improved finite-segment method for analyzing shear lag effect in thin-walled box girders[J]. *Journal of Structural Engineering*, 2012, **138**(10): 1279-1284.
- [5] ZHOU Shi-jun. Finite beam element considering shear-lag effect in box girder[J]. *Journal of Engineering Mechanics*, 2010, **136**(9): 1115-1122.
- [6] 刘世忠, 欧阳永金, 吴亚平, 夏旻. 变截面薄壁箱梁剪力滞剪切变形效应分析[J]. 中国公路学报, 2002, **15**(3): 61-66. (LIU Shi-zhong, OUYANG Yong-jin, WU Ya-ping, XIA Ming. Non-uniform thin wall box analysis of considering both shear lag and shear deformation[J]. *China Journal of Highway and Transport*, 2002, **15**(3): 61-66. (in Chinese))
- [7] 吴亚平. 薄壁箱梁剪力滞后及剪切变形双重效应分析[C]//第三届全国结构工程学术会议论文集. 1994: 425-428. (WU Ya-ping. Analysis on shear lag effect and shear deformation of thin walled box girder[C]//*Proceedings of the Third National Conference on Structural Engineering*. 1994: 425-428. (in Chinese))
- [8] 曾有凤. 箱型梁剪力滞和剪切变形双重效应研究[D]. 硕士学位论文. 南宁: 广西大学, 2014: 40-62. (ZENG You-feng. Investigation on shear deformation and shear lag effects on box-girders[D]. Master Thesis. Nanning: Guangxi University, 2014: 40-62. (in Chinese))
- [9] 吴幼明, 罗旗帜, 岳珠峰. 薄壁箱梁剪力滞效应的能量变分法[J]. 工程力学, 2003, **20**(4): 160, 161-165. (WU You-ming, LUO Qi-zhi, YUE Zhu-feng. Energy-variational method of the shear lag effect in thin walled box girder[J]. *Engineering Mechanics*, 2003, **20**(4): 160, 161-165. (in Chinese))
- [10] 丁南宏, 林丽霞, 钱永久. 变截面箱梁剪力滞及剪切变形效应近似计算方法[J]. 铁道科学与工程学报, 2011, **8**(1): 14-18. (DING Nan-hong, LIN Li-xia, QIAN Yong-jiu. An approximate method to analyze the effect of shear lag and shear deformation of box beam with varying depth[J]. *Journal of Railway Science and Engineering*, 2011, **8**(1): 14-18. (in Chinese))
- [11] 周茂定, 李丽园, 张元海. 考虑剪切变形时薄壁箱梁的挠曲分析[J]. 工程力学, 2015, **32**(10): 138-144. (ZHOU Mao-ding, LI Li-yuan, ZHANG Yuan-hai. Flexural analysis of thin-walled box girders with shear deformation[J]. *Engineering Mechanics*, 2015, **32**(10): 138-144. (in Chinese))
- [12] S·铁摩辛柯, J·盖莱. 材料力学[M]. 胡人礼, 译. 北京: 科学出版社, 1978: 256-264. (Timoshenko S, Gere J. *Mechanics of Materials*[M]. HU Ren-li, transl. Beijing: Science Press, 1978: 256-264. (Chinese version))
- [13] 吴幼明, 罗旗帜. 一类二阶常系数微分方程组的通解[J]. 佛山科学技术学院学报(自然科学版), 2002, **20**(2): 10-14. (WU You-ming, LUO Qi-zhi. The general solutions to one kind of systems of second order ordinary differential equation with constant coefficients[J]. *Journal of Foshan University (Natural Science Edition)*, 2002, **20**(2): 10-14. (in Chinese))

- [14] 牟兆祥. 基于能量变分原理的薄壁箱梁剪力滞效应解析法研究[D]. 硕士学位论文. 长沙: 中南大学, 2014: 12-113. (MOU Zhao-xiang. Analytical study on shear lag effect of thin-walled box girder based on energy-variational principle[D]. Master Thesis. Changsha: Central South University, 2014: 12-113. (in Chinese))
- [15] 武建华, 郑辉中, 古滨. 材料力学[M]. 重庆: 重庆大学出版社, 2008: 388-390. (WU Jian-hua, ZHENG Hui-zhong, GU Bin. *Mechanics of Materials* [M]. Chongqing: Chongqing University Press, 2008: 388-390. (in Chinese))

Analysis on Shear Deformation and Shear-lag Effects on Twin-Cell Box Girders

ZHANG Hui^{1,2}, ZHANG Yu-yuan², ZHANG Yuan-hai², LI Wei³

(1. Key Laboratory of Road & Bridge and Underground Engineering of Gansu Province,

Lanzhou Jiaotong University, Lanzhou 730070, P.R.China;

2. School of Civil Engineering, Lanzhou Jiaotong University,

Lanzhou 730070, P.R.China;

3. Southwest Jiaotong University, Chengdu 614202, P.R.China)

Abstract: Based on the flanges' different maximum shear angle differences selected as the shear-lag generalized displacements, the energy variational principle was applied to deduce the shear-lag differential equations for twin-cell box girders with and without shear deformation in consideration, and the initial parametric solutions of the box girder's longitudinal stress and vertical deflection were given according to the boundary conditions. From the angle of mechanics and mathematics it was proved that the shear deformation and the shear lag were 2 relatively independent mechanical behaviors, of which the impacts on the box girder mechanics were expounded: the shear deformation had no effect on the longitudinal stress but had great influence on the vertical deflection. The example of a simply-supported box girder shows that the longitudinal stress at the middle cross section calculated with the presented analytic method and with the numerical method are in good agreement, of which the lateral distribution is similar to that in the case of single-cell box girders; however, the shear-lag effect around the side webs is slightly greater than that around the middle web. The shear deformation adds to the middle deflection of the box girder under concentrated and uniformly distributed loads by 4.6% and 2.7%, respectively.

Key words: twin-cell box girder; shear-lag effect; shear deformation; energy variational method; finite element

Foundation item: The National Natural Science Foundation of China (51508255; 51468032; 51268029)

引用本文/Cite this paper:

张慧, 张玉元, 张元海, 李巍. 单箱双室简支箱梁剪切变形及剪力滞双重效应分析[J]. 应用数学和力学, 2016, 37(8): 791-803.

ZHANG Hui, ZHANG Yu-yuan, ZHANG Yuan-hai, LI Wei. Analysis on shear deformation and shear-lag effects on twin-cell box girders[J]. *Applied Mathematics and Mechanics*, 2016, 37(8): 791-803.